4

The effect of temperature on chemosensory cilia and intraflagellar transport in *C. elegans*

Jona Mijalkovic, Miranda Little and Erwin J.G. Peterman

In preparation

Abstract

Non-motile cilia are organelles that act as the cell's antennae to detect changes in the extracellular environment. They are built and maintained by a bidirectional, microtubule-based, motor-driven process called intraflagellar transport (IFT). In this chapter, we probe the response of the IFT machinery to temperature (21-35°C) using fluorescence microscopy of labeled IFT-dynein motors and tubulin in living *C. elegans*. We find only a mild effect on anterograde, and no effect on retrograde IFT-train velocities. At high temperatures, IFT dynein redistributes within the cilium, while the microtubule axoneme stays intact. Our results reveal a reversible uncoupling between motility and cilium length maintenance in the thermal ciliary response.

4.1 Introduction

Cilia are microtubule-based organelles that are found on the surface of most eukaryotic cells and play a role in sensory perception and signaling [1, 2]. They are assembled and maintained by a bidirectional transport process along microtubules called intraflagellar transport (IFT) [3]. In *C. elegans*, plus-end-directed kinesin-2 motors drive anterograde transport from the ciliary base to the distal tip [4-6], whereas minus-end-directed IFT dynein motors return cargo from the tip to the base [7]. Although cilia are recognized to play a role in sensory perception, little is known about the response of the IFT machinery to extracellular stimuli.

Thermal stimuli are detected by sensory neurons and converted to changes in ion currents [8]. Behavioral traits and signaling pathways underlying *C. elegans* thermosensation are relatively well understood [9, 10]. Unlike mammals, which have internal homeostasis regulation mechanisms, *C. elegans* uses complex, experience-dependent behavioral patterns to regulate its body temperature. This temperature-guided motion, called thermotaxis, enables worms to move along temperature gradients and detect temperature changes with very high (~0.05°C) sensitivity [11-13]. At the cellular level, laser ablation [14, 15] and genetic [16] studies have identified AFD, an amphid sensory neuron, as the major thermosensory neuron in *C. elegans*. *In vivo* patch-clamp recordings have shown that temperature modulates the opening and closing of cyclic nucleotide-gated (CNG) ion channels in AFD neurons [8]. The AFD thermosensation signaling cascade additionally involves cGMP, transmembrane guanylate cyclases and Ca^{2+} [17-19]. Although the amphid neuron response to temperature has been systematically investigated, the role of the phasmid neuron remains elusive [14, 20, 21]. Moreover, little is known about how temperature affects ciliary structure and motor-driven transport.

There is evidence that signaling proteins are localized in the cilium and some have been shown to, at least part of the time, undergo IFT [22]. Furthermore, transient receptor potential (TRP) channels, which are the primary

temperature sensors in mammals, are expressed in *C. elegans* phasmid and OLQ cilia and are transported by IFT [23, 24]. These findings raise the possibility of IFT involvement in thermosensation. In addition, biochemical processes underlying IFT are affected by temperature. The assembly of tubulin-GTP complexes into microtubules, which form the ciliary axoneme track for IFT motors, is temperature-dependent. Polymerization can be induced by higher temperatures, whereas reversal of polymerization occurs at lower temperatures [25-27]. IFT motors kinesin-2 and IFT dynein are driven by an enzymatic, temperature-dependent process of ATP binding, hydrolysis and phosphate release. *In vitro* optical tweezers bead experiments [28, 29] and gliding assays [30] have shown that kinesin-1-driven gliding velocity follows the Arrhenius law up to 30-35°C. Mammalian dynein similarly exhibits *in vitro* Arrhenius-like temperature dependence above 15°C, but *in vivo* reports are lacking.

Here, we probed the temperature-dependence of IFT in *C. elegans* phasmid cilia using fluorescence microscopy of labeled IFT-dynein motors and tubulin. We observed a temperature effect on anterograde, but not retrograde, velocities. We also found that heating induces a reversible retraction of motors towards the base and transition zone, while the ciliary axoneme is unaffected. Our results uncover a ciliary response to stimulus in which motors respond independently of their track. This thermal response is different from the response observed to chemical stimuli [31].

4.2 Results

To investigate how phasmid cilia and IFT respond to temperature, we incubated *C. elegans* young adults in pre-heated sample chambers at 21°C, 25°C, 30°C and 35°C (Figure 4.1A). To avoid developmental or memory-dependent differences in thermal response, the cultivation temperature of all worms was kept constant at 20°C prior to the measurements [11]. Following 10-minute exposure to each temperature, we recorded fluorescence image sequences of the IFT-dynein marker XBX-1::EGFP [32-34] and subsequently generated summed fluorescence images (Figure 4.1A) to determine the temperature dependence of the distribution of the motors along the cilium (Figure 4.1B) [35]. At 21°C, IFT dynein is distributed along the entire ciliary axoneme with some accumulation at the base and transition zone (Figure 4.1A,B), congruent with previous reports [32]. The same distribution is observed at 25°C. At temperatures above 25°C, however, IFT-dynein motors appear to extend less far from the ciliary base (16 ± 9% at 30°C (average ± s.e.m.; n=15) and 47 ± 12% at 35°C (n=10)), s.e.m.) (Figure 1B,C), while substantially more motors appear to be present at the base. At 35°C, IFT dynein occupies only 64 ± 12% of the 21°C length and appears completely retracted from the distal segment.

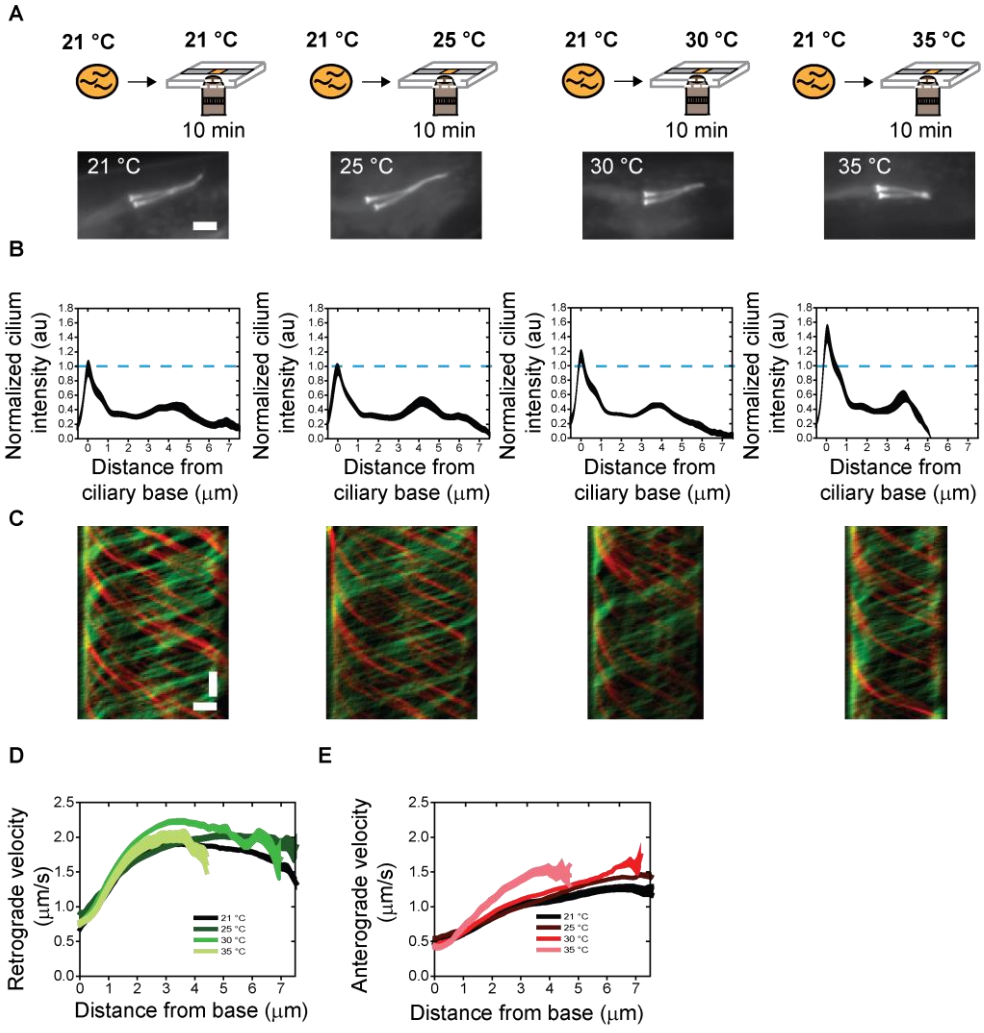

Figure 4.1: IFT response to temperature increase in *C. elegans* phasmid neurons

A. Schematic diagram of the temperature assay and representative summed fluorescence images (obtained from 150 subsequent image frames) of XBX-1::EGFP in phasmid cilia. Scale bar: 2 μm. **B.** Normalized, background-corrected, summed XBX-1 cilium fluorescence intensity at 21°C (n=13), 25°C (n=12), 30°C (n=15), 35°C (n=10). Line thickness is s.e.m.. The dotted line indicates maximum cilium fluorescence intensity at 21°C as a visual aid. **C.**

XBX-1::EGFP kymographs showing retrograde (green) and anterograde (red) motility. Time: vertical; scale bar 2 s. Position: horizontal; scale bar 2 μm. Kymographs correspond to the cilia shown in (B). **D.** Average retrograde velocity at 21°C (n=24 cilia; 176 trains), 25°C (n=7 cilia; 62 trains), 30°C (n=21 cilia; 163 trains), 35°C (n=17 cilia; 96 trains). Line thickness is s.e.m.. **E.** Average anterograde velocity at 21°C (n=24 cilia; 239 trains), 25°C (n=7 cilia; 62 trains), 30°C (n=21 cilia; 202 trains), 35°C (n=17 cilia; 92 trains). Line thickness is s.e.m..

It is well established that IFT dynein is the sole driver of retrograde (tip to base) IFT in *C. elegans* phasmid cilia. IFT dynein is brought to the tip as cargo by kinesin-2 driven anterograde transport (base to tip). In order to probe how the dynamics of IFT is affected by temperature, we extracted Fourier-filtered kymographs from the sequences using *KymographClear* (Figure 4.1C). From these kymographs location-dependent anterograde and retrograde velocities were extracted using *KymographDirect* (Figure 4.1D,E) [35]. At 21°C, the measured retrograde (Figure 4.1C,D) and anterograde (Figure 4.1C,E) velocity profiles correspond well with previous reports [5, 6, 36]. Intriguingly, at temperatures up to 30°C the motor velocity does not appear to be affected substantially (Figure 4.1C-E). At 35°C, however, the anterograde, but not retrograde, velocity is significantly higher (Figure 4.1C-E), suggesting that kinesin-2 and IFT-dynein motors are affected differently by temperature *in vivo*. The anterograde velocity change is particularly evident in the 'handover zone' at 2-4 μm, where kymographs reveal a sharper transition of IFT trains from the base and transition zone to the proximal segment (Figure 4.1C). In this region, a relay between the two kinesins that drive anterograde transport takes place as kinesin-II gradually docks off IFT trains and OSM-3 docks on [5]. Our results suggest that the kinesin-II-to-OSM-3 handover could be affected directly, by altered rates of motors detaching from and attaching to IFT trains, or

indirectly, by a temperature-induced imbalance of kinesin-II and OSM-3 velocities.

To probe whether the temperature-induced motor retraction and velocity changes are reversible, we performed temperature-ramp experiments. Animals grown at 21°C were incubated for 10 minutes sequentially at 21°C, 25°C, 30°C and 35°C. (Figure 4.2A). The XBX-1 distributions observed in these temperature-ramp experiments (Figure 4.2A) were very similar to those observed in the single temperature experiments (Figure 4.1), indicating that the response to temperature takes place within minutes. After the 10-minute incubation at the highest temperature, animals were placed again at 21°C for an hour and motor distribution (Figure 4.2A), retrograde velocity (Figure 4.2B) and anterograde velocity (Figure 4.2C) were determined, yielding results indistinguishable from experiments on animals that had only experienced 21°C (Figure 4.1B, D, and E). These observations indicate that the response of IFT to temperatures up to 35°C is reversible.

Since IFT motors require microtubules as a track, we asked whether the motor redistribution observed at 30°C and above is due to a temperature-induced (partial) collapse of the ciliary axoneme. To test this, we subjected animals expressing fluorescently labeled cilium-specific tubulin (TBB-4::EGFP) to the temperature ramps applied above (Figure 4.2A, D). Remarkably, in contrast to the observed IFT-dynein redistribution, axoneme length did not appear to be affected at any of the temperatures applied (Figure 4.2A, D).

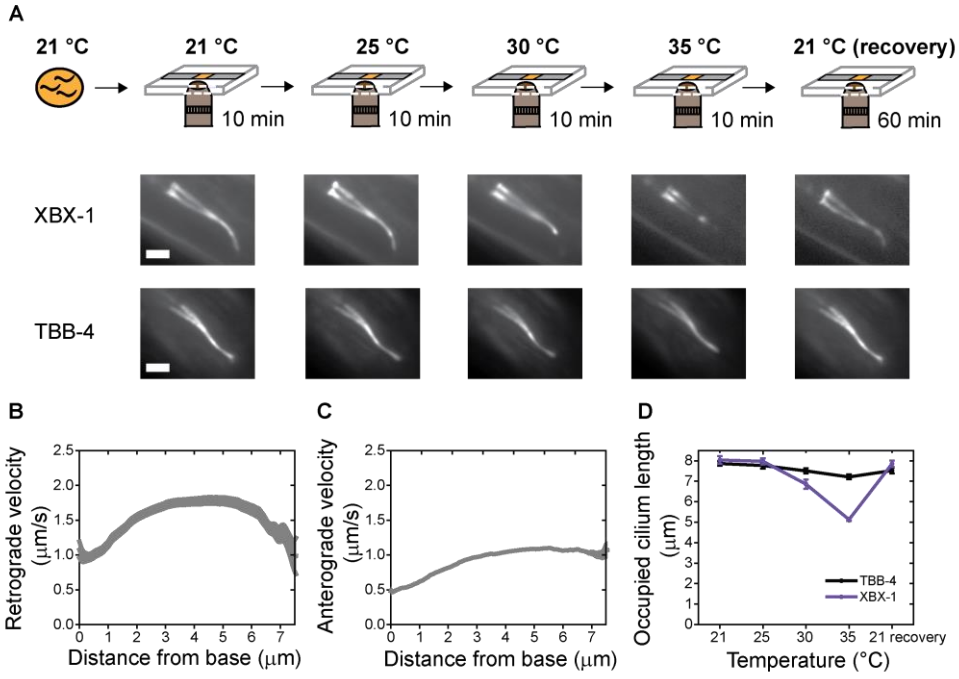

Figure 4.2: IFT response to temperature increase is reversible

A. Top: Schematic diagram of sequential 10-minute incubations in stage heater chambers at 21°C, 25°C, 30°C and 35°C, followed by 1 hour recovery at 21°C. Bottom: Representative summed fluorescence images (obtained from 150 subsequent image frames) of XBX-1::EGFP and TBB-4::EGFP in phasmid cilia. Scale bar: 2μm. **B.-C.** Average XBX-1 retrograde (B; n=10 cilia; 69 trains) and anterograde (C; n=10 cilia; 83 trains) recovery velocity at 21°C. Line thickness is s.e.m.. **D.** Cilium length (black, TBB-4) and cilium length occupied by motors (purple, XBX-1) at each temperature. Error is s.e.m..

4.3 Discussion

Non-motile cilia act as cellular sensory hubs to detect and respond to extracellular stimuli such as odorants and osmotic change. *Chlamydomonas* flagella retain IFT but reversibly shorten to approximately half of their length when exposed to different potassium or sodium concentrations [31, 37] *C. elegans* cilia similarly retract in response to laser-induced dendritic perturbation (Chapter 6). Here, we observe a response to thermal stimuli characterized by retraction of only motors and not the ciliary axoneme. The apparent uncoupling between motor occupancy and axonemal length is striking given that IFT dynein and kinesin are responsible for maintaining their track, raising questions about how the ciliary axoneme can stay intact while the IFT motors retract. Our findings can be explained by the temperature-dependence of tubulin dynamics. *In vitro* studies have shown that high temperatures favor polymerization, while low temperatures favor depolymerization [25]. At the time scale of our experiments (tens of minutes), the increased stability of the axoneme at 30°C and 35°C likely prevents retraction despite the IFT motor response.

In vitro gliding assay experiments on kinesin-1 reveal an Arrhenius-like 3-fold velocity and ATPase activity increase at 25°C and 4-fold increase at 30°C [30]. A recent study observed a ~2-fold kinesin-1 velocity increase from 22°C to 27°C [29]. We, however, find a kinesin-2 temperature dependence only above 30°C. Additionally, whereas *in vitro* experiments demonstrate a ~2-fold increase in dynein velocity from 27°C to 30°C, we observe no significant temperature dependence change *in vivo*. Our results suggest that there is a difference in ATPase activity between motor families, or between *in vitro* and *in vivo*-acting motors. Temperature modulation *in vivo* is likely to be different due to the collective behavior of motors, as well as the presence of co-factors and regulators which could play additional roles in the thermal response.

In summary, we have shown that IFT in phasmid cilia is temperature-dependent. Kinesin-2, but not IFT-dynein velocities are affected. Additionally, at high temperatures IFT motors redistribute within the cilium whilst the ciliary axoneme stays intact. Our results reveal an uncoupling between motility and ciliary maintenance in the thermal ciliary response.

4.4 Materials and methods

C. elegans maintenance and strains

C. elegans strains were cultivated with OP-50 *E.coli* and maintained at 20°C using standard procedures. The strains were constructed using Mos1 Mediated Single Copy Insertion (MosSCI) as described previously [5, 36, 38].

Sample preparation and imaging

C. elegans young adult hermaphrodites were anaesthetized in 5 mM levamisole in M9 and immobilized on a 2% agarose in M9 pad covered with a 22 × 22 mm cover glass and sealed with VaLaP. The imaging slides were mounted on a holder inside a stage top incubator (Tokai Hit) prior to setting the incubator and objective temperature to 21°C, 25°C, 30°C or 35°C. For the temperature-ramp experiments, the incubator temperature was sequentially increased from 21°C to 35°C, followed by a 1-hour recovery at 21°C. The temperature was confirmed using a sensitive thermometer positioned on top of the imaging slide. Fluorescence images were obtained using a custom-built epi-illuminated fluorescence microscope described in detail in Prevo *et al* [5]. 150 frames were recorded for each phasmid cilium at 152ms per frame and 300 EM gain and laser power was kept constant for both strains.

Image analysis

Images were analyzed using KymographDirect and KymographClear [35]. Cilium length and cilium length occupied by motors were determined using the average, background-corrected cilium fluorescence intensity.

4.5 Acknowledgements

We acknowledge financial support from the Netherlands Organization for Scientific Research (NWO) via a Vici grant (E.J.G.P).

4.6 Author contributions

Conceptualization, J.M. and E.J.G.P.; Investigation, J.M. and M.L.; Formal Analysis, J.M.; Writing – Original Draft, J.M; Writing – Review & Editing, J.M. and E.J.G.P.; Funding Acquisition, E.J.G.P; Supervision, E.J.G.P.

4.7 References

1. Nachury, M.V. How do cilia organize signalling cascades? *Philosophical transactions of the Royal Society of London. Series B, Biological sciences* **369** (2014).
2. Singla, V. & Reiter, J.F. The primary cilium as the cell's antenna: signaling at a sensory organelle. *Science (New York, N.Y.)* **313**, 629-633 (2006).
3. Ishikawa, H. & Marshall, W.F. Ciliogenesis: building the cell's antenna. *Nature reviews. Molecular cell biology* **12**, 222-234 (2011).
4. Pan, X. *et al.* Mechanism of transport of IFT particles in C. elegans cilia by the concerted action of kinesin-II and OSM-3 motors. *The Journal of cell biology* **174**, 1035-1045 (2006).
5. Prevo, B., Mangeol, P., Oswald, F., Scholey, J.M. & Peterman, E.J. Functional differentiation of cooperating kinesin-2 motors orchestrates cargo import and transport in C. elegans cilia. *Nature cell biology* **17**, 1536-1545 (2015).
6. Snow, J.J. *et al.* Two anterograde intraflagellar transport motors cooperate to build sensory cilia on C. elegans neurons. *Nature cell biology* **6**, 1109-1113 (2004).
7. Signor, D. *et al.* Role of a class DHC1b dynein in retrograde transport of IFT motors and IFT raft particles along cilia, but not dendrites, in chemosensory neurons of living Caenorhabditis elegans. *The Journal of cell biology* **147**, 519-530 (1999).
8. Ramot, D., MacInnis, B.L. & Goodman, M.B. Bidirectional temperature-sensing by a single thermosensory neuron in C. elegans. *Nature neuroscience* **11**, 908-915 (2008).
9. Aoki, I. & Mori, I. Molecular biology of thermosensory transduction in C. elegans. *Current opinion in neurobiology* **34**, 117-124 (2015).
10. Garrity, P.A., Goodman, M.B., Samuel, A.D. & Sengupta, P. Running hot and cold: behavioral strategies, neural circuits, and the molecular machinery for thermotaxis in C. elegans and Drosophila. *Genes & development* **24**, 2365-2382 (2010).
11. Hedgecock, E.M., Russel, R.L. Normal and mutant thermotaxis in the nematode Caenorhabditis elegans. *Proceedings of the National Academy of Sciences of the United States of America* **72**, 4061-4065 (1975).
12. Clark, D.A., Biron, D., Sengupta, P. & Samuel, A.D. The AFD sensory neurons encode multiple functions underlying thermotactic behavior in Caenorhabditis elegans. *The Journal of neuroscience : the official journal of the Society for Neuroscience* **26**, 7444-7451 (2006).
13. Ryu, W.S. & Samuel, A.D. Thermotaxis in Caenorhabditis elegans analyzed by measuring responses to defined Thermal stimuli. *The Journal of neuroscience : the official journal of the Society for Neuroscience* **22**, 5727-5733 (2002).
14. Mori, I. & Ohshima, Y. Neural regulation of thermotaxis in Caenorhabditis elegans. *Nature* **376**, 344-348 (1995).

15. Chung, S.H., Clark, D.A., Gabel, C.V., Mazur, E. & Samuel, A.D. The role of the AFD neuron in C. elegans thermotaxis analyzed using femtosecond laser ablation. *BMC neuroscience* **7**, 30 (2006).
16. Perkins, L.A., Hedgecock, E.M., Thomson, J.N. & Culotti, J.G. Mutant sensory cilia in the nematode Caenorhabditis elegans. *Developmental biology* **117**, 456-487 (1986).
17. Wasserman, S.M., Beverly, M., Bell, H.W. & Sengupta, P. Regulation of response properties and operating range of the AFD thermosensory neurons by cGMP signaling. *Current biology : CB* **21**, 353-362 (2011).
18. Kimura, K.D., Miyawaki, A., Matsumoto, K. & Mori, I. The C. elegans thermosensory neuron AFD responds to warming. *Current biology : CB* **14**, 1291-1295 (2004).
19. Inada, H. *et al.* Identification of guanylyl cyclases that function in thermosensory neurons of Caenorhabditis elegans. *Genetics* **172**, 2239-2252 (2006).
20. Beverly, M., Anbil, S. & Sengupta, P. Degeneracy and neuromodulation among thermosensory neurons contribute to robust thermosensory behaviors in Caenorhabditis elegans. *The Journal of neuroscience : the official journal of the Society for Neuroscience* **31**, 11718-11727 (2011).
21. Kuhara, A. *et al.* Temperature sensing by an olfactory neuron in a circuit controlling behavior of C. elegans. *Science (New York, N.Y.)* **320**, 803-807 (2008).
22. Ye, F. *et al.* Single molecule imaging reveals a major role for diffusion in the exploration of ciliary space by signaling receptors. *eLife* **2**, e00654 (2013).
23. Qin, H. *et al.* Intraflagellar transport is required for the vectorial movement of TRPV channels in the ciliary membrane. *Current biology : CB* **15**, 1695-1699 (2005).
24. Palkar, R., Lippoldt, E.K. & McKemy, D.D. The molecular and cellular basis of thermosensation in mammals. *Current opinion in neurobiology* **34**, 14-19 (2015).
25. Borisy, G.G., Marcum, J.M., Olmsted, J.B., Murphy, D.B. & Johnson, K.A. Purification of tubulin and associated high molecular weight proteins from porcine brain and characterization of microtubule assembly in vitro. *Annals of the New York Academy of Sciences* **253**, 107-132 (1975).
26. Olmsted, J.B., Marcum, J.M., Johnson, K.A., Allen, C. & Borisy, G.G. Microtuble assembly: some possible regulatory mechanisms. *Journal of supramolecular structure* **2**, 429-450 (1974).
27. Fygenson, D.K., Braun, E. & Libchaber, A. Phase diagram of microtubules. *Physical review. E, Statistical physics, plasmas, fluids, and related interdisciplinary topics* **50**, 1579-1588 (1994).
28. Kawaguchi, K. & Ishiwata, S. Temperature dependence of force, velocity, and processivity of single kinesin molecules. *Biochemical and biophysical research communications* **272**, 895-899 (2000).
29. Hong, W., Takshak, A., Osunbayo, O., Kunwar, A. & Vershinin, M. The Effect of Temperature on Microtubule-Based Transport by Cytoplasmic Dynein and Kinesin-1 Motors. *Biophysical journal* **111**, 1816 (2016).

30. Bohm, K.J., Stracke, R., Baum, M., Zieren, M. & Unger, E. Effect of temperature on kinesin-driven microtubule gliding and kinesin ATPase activity. *FEBS letters* **466**, 59-62 (2000).
31. Solter, K.M. & Gibor, A. The relationship between tonicity and flagellar length. *Nature* **275**, 651-652 (1978).
32. Mijalkovic, J., Prevo, B., Oswald, F., Mangeol, P. & Peterman, E.J. Ensemble and single-molecule dynamics of IFT dynein in Caenorhabditis elegans cilia. *Nature communications* **8**, 14591 (2017).
33. Wei, Q. *et al.* The BBSome controls IFT assembly and turnaround in cilia. *Nature cell biology* **14**, 950-957 (2012).
34. Burghoorn, J. *et al.* Dauer pheromone and G-protein signaling modulate the coordination of intraflagellar transport kinesin motor proteins in C. elegans. *Journal of cell science* **123**, 2077-2084 (2010).
35. Mangeol, P., Prevo, B. & Peterman, E.J. KymographClear and KymographDirect: two tools for the automated quantitative analysis of molecular and cellular dynamics using kymographs. *Molecular biology of the cell* (2016).
36. Mijalkovic, J., Prevo, B., Oswald, F., Mangeol, P.J.J. & Peterman, E.J.G. Quantification of IFT-Dynein Dynamics in C.elegans. *Biophysical journal* **108**, 134a.
37. Lefebvre, P.A., Nordstrom, S.A., Moulder, J.E. & Rosenbaum, J.L. Flagellar elongation and shortening in Chlamydomonas. IV. Effects of flagellar detachment, regeneration, and resorption on the induction of flagellar protein synthesis. *The Journal of cell biology* **78**, 8-27 (1978).
38. Frokjaer-Jensen, C. *et al.* Single-copy insertion of transgenes in Caenorhabditis elegans. *Nature genetics* **40**, 1375-1383 (2008).